Available online at www.sciencedirect.com
SCIENCE DIRECT®
Journal of Sound and Vibration 275 (2004) 739–755
JOURNAL OF SOUND AND VIBRATION
www.elsevier.com/locate/jsvi

Acoustic wave reflection from a rough seabed with a continuously varying sediment layer overlying an elastic basement

Jin-Yuan Liu*, Sheng-Hsiung Tsai, Chau-Chang Wang, Chung-Ray Chu

Institute of Undersea Technology, National Sun Yat-sen University, 70 Lian-Hae Road, Kaohsiung 804, Taiwan

Received 17 May 2002; accepted 26 June 2003

Abstract

Acoustic plane wave interactions with a rough seabed with a continuously varying density and sound speed in a fluid-like sediment layer overlying an elastic basement is considered in this paper. The sediment layer possesses a generalized exponential type of variation in density and one of the three classes of sound speed profiles, which are constant, k^2-linear, or inverse-square variations. Analytical solutions for the Helmholtz equation in the sediment layer, combined with a formulation based upon boundary perturbation theory, facilitate numerical implementation for the solution of coherent field. The coherent reflection coefficients corresponding to the aforementioned density and sound speed profiles for various frequencies, roughness parameters, basement stiffness, are numerically generated and analyzed. Physical interpretations are provided for various results. The proposed model characterizes three important features of a realistic sea floor, including seabed roughness, sediment inhomogeneities, and basement shear property, therefore, provides a canonical environmental model for the study of seabed acoustics.

1. Introduction

The problem of acoustic wave interactions with sea floor has long been a subject of interest in underwater sound, and is a major issue in seabed acoustics, particularly in recent pursuit of geoacoustic inversion. The sea floor contains many important features affecting acoustic propagation in oceans, among others, the seabed roughness, sediment inhomogeneities, and basement shear property, may need to be considered one way or another, in order to cover a wide range of frequency. Here, to illustrate the combined effects of the above-mentioned characteristics

*Corresponding author. Tel.: 886-7-5252000; fax: 866-7-5255277.
E-mail address: jimliu@mail.nsysu.edu.tw (J.-Y. Liu).

0022-460X/$ - see front matter © 2003 Elsevier Ltd. All rights reserved.
doi:10.1016/j.jsv.2003.06.012

on acoustic interactions with the sea floor, we consider a simplest problem, i.e., a plane wave interacting with such a sea floor; the overall environmental model is shown in Fig. 1. The special features of the model include: (1) the seabed is rough, (2) the acoustic properties of the fluid-like sediment vary continuously throughout the layer, and (3) the sea floor basement is an elastic medium. Although, the problem is not completely new in the sense that several individual aspects of the problem have been studied previously [1–5], however, those analyses were either limited or incompleted (e.g., Ref. [2] only considers one type of the sound-speed profiles, and Refs. [3–5] does not include seabed roughness and basement shear property), so that an integrated analysis seems to be in order.

The present analysis in effect is a problem of acoustic wave propagation and scattering from rough interfaces in a horizontally stratified medium, a subject that has raised many interests in the past two decades in ocean acoustics, and many theories and numerical algorithms have thus been developed, for example, the spectral or wavenumber integration method [1,6,7], the normal mode method [8–10], and the parabolic equation method [11,12], etc.; these are well documented in Ref. [13]. In practice, the present problem may completely be taken care of by a numerical approach. However, in some cases, the Helmholtz equation for certain classes of sediments with varying density and/or sound speed may permit exact solutions, and very often, these solutions are directly applicable to a realistic environment. Under this situation, the exact solutions not only are beneficial to the analysis per se, but also shed light on the correctness of numerical schemes, making the search of the analytical solutions for the Helmholtz equation a constant interest.

In this regard, there are several well-known examples. For instance, for variable sound speed with constant density, the Helmholtz equation may be solved for the Epstein profile [14], the linear profile [15], and the k^2-linear profile [16]. For isovelocity layer, an exponential profile for density is frequently employed [17–21]. Recently, a generalized exponential density profile, jointly with a constant, k^2-linear, or inverse-square sound speed profile have been investigated in a sequence of papers by Robins for a plane wave interacting with such a transition layer bounded by unperturbed interfaces [3–5,22]; these density and sound speed profiles provide a model close to realistic sediment layer [23], so that they are to be applied in this study.

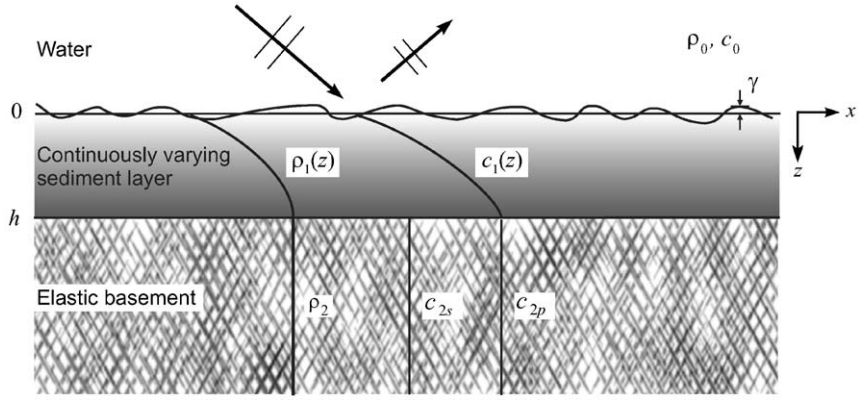

Fig. 1. A plane wave incident upon a two-dimensional rough seabed with a fluid-like sediment layer, possessing a continuous increase of density and sound speed, overlying a uniform elastic basement.

In terms of the overall analysis, none of the above-mentioned studies has included seabed roughness, variable sediment, and basement shear property, simultaneously. Furthermore, the results corresponding to the generalized exponential density profile associated with the inverse-square sound speed profile are still limited due to a difficulty in the numerical treatment for the involved special functions [4]. The present study shall take up a complete analysis on the coherent reflection coefficients for various profiles, and the results are useful in the modelling of seabed acoustics.

2. Formulations

Consider a monotonic acoustic plane wave with time dependence $e^{-i\omega t}$, propagating on the x–z plane in a uniform fluid medium with density ρ_0 and sound speed c_0, impinging upon a one-dimensional rough seabed with random elevation $\gamma(x)$, as shown in Fig. 1. The sediment layer of thickness h is considered to be fluid-like, with both density $\rho_1(z)$ and sound speed $c_1(z)$ varying continuously with depth in a certain fashion, which is to be specified later. The basement is assumed to be a uniform elastic semi-infinite medium with density ρ_2, compressional sound speed c_{2p}, and shear sound speed c_{2s}.

2.1. Helmholtz equations and boundary conditions

For the environmental model shown in Fig. 1, the Helmholtz equations for acoustic or seismic waves in various layers are [16]

$$(\nabla^2 + k_0^2)p_0 = 0, \tag{1}$$

$$(\nabla^2 + k_1^2)p_1 = \frac{1}{\rho_1}\frac{\mathrm{d}\rho_1}{\mathrm{d}z}\frac{\partial p_1}{\partial z}, \tag{2}$$

$$(\nabla^2 + k_{2p}^2)\phi_2 = 0, \tag{3}$$

$$(\nabla^2 + k_{2s}^2)\psi_2 = 0, \tag{4}$$

where p_i is the acoustic pressure in layer i, and ϕ_2 and ψ_2 represent the displacement potentials for compressible and shear wave in the basement, respectively. The medium wavenumber is defined as $k_i = \omega/c_i$, and is function of z in the sediment layer. It is noted that the term on the right-hand side of Eq. (2) represents the effects of density variation in the medium.

The boundary conditions imposed by the physical constraints are

$$w_0|_{z=\gamma} = w_1|_{z=\gamma}, \tag{5}$$

$$p_0|_{z=\gamma} = p_1|_{z=\gamma}, \tag{6}$$

$$w_1|_{z=h} = w_2|_{z=h}, \tag{7}$$

$$p_1|_{z=h} = -\sigma_{zz,2}|_{z=h}, \tag{8}$$

$$0 = \sigma_{rz,2}|_{z=h}, \tag{9}$$

where w_i's and σ_i's are, respectively, outward normal displacement and stress; γ and h are, respectively, the random roughness elevation and the thickness of the sediment layer. The relationship between these physical quantities and the displacement potentials are well documented and may be easily found in literature, e.g., Ref. [24].

It is clear that, since γ is random, the acoustic fields in various layers are also random. Under the framework of boundary perturbation analysis, the total field may be separated into a deterministic coherent field and a random scattered field. According to the theory developed by Kuperman and Schmidt [1], which is to be employed in later analysis, the coherent field may be expressed in terms of a few operators involving only the problem for plane interfaces; these operators effectively account for the scattering loss incurred by the surface roughness.

With this in mind, we shall first formulate the problem for wave propagation in a horizontally stratified medium with unperturbed interfaces, and then invoke the boundary perturbation formulation to solve for the coherent reflection field.

2.2. Exact solutions of the Helmholtz equation in a continuously varying sediment layer

To proceed the analysis, the acoustic fields in the various layers should first be obtained. Since the upper and the lower layers are uniform, the solutions are simply the exponential functions. However, the solution of Eq. (2) for an arbitrary variation of density and/or sound speed generally requires numerical procedure. Here, we are interested in the analytical solutions corresponding to various combinations of density and sound speed profiles which are geologically meaningful.

Under this consideration, it has been shown that the exact solutions of Eq. (2) may exist if the density and the sound speed profiles satisfy the following combinations [8,15,20,21]:

$$\rho(z) = \frac{A\mathrm{e}^{\alpha z}}{(\mathrm{e}^{\alpha z} + a)^2}, \quad \text{generalized exponential}, \tag{10}$$

$$\frac{1}{c^2(z)} = \begin{cases} \frac{1}{\check{c}_1^2}, & \text{constant}, \\ \frac{(1+\delta z)}{\check{c}_1^2}, & k^2\text{-linear}, \\ \frac{b^2}{\check{c}_0^2} + \left(\frac{1}{\check{c}_1^2} - \frac{b^2}{\check{c}_0^2}\right)\frac{1}{(1-\kappa z)^2}, & \text{inverse-square}, \end{cases} \tag{11}$$

where $A, \alpha, a, \check{c}_1, \delta, b, \check{c}_0$, and κ are constants, which when appropriately assigned may well fit the profiles in a realistic sea floor [23]; an example of the profiles is shown in Fig. 2.

For a plane wave having the horizontal wavenumber $k_x = k_0 \cos\theta_0 = k_i \cos\theta_i$, with θ_0 being the incident grazing angle, the solution of Eq. (2) may be expressed as

$$p_1(x, z) = \tilde{p}_1(z)\mathrm{e}^{\mathrm{i}k_x x}. \tag{12}$$

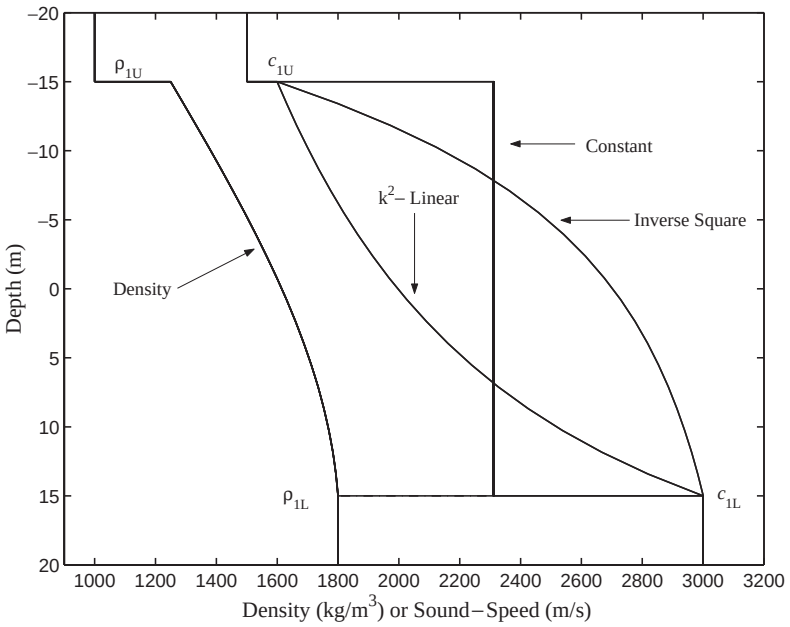

Fig. 2. Sample profiles for density and sound speed; values for various parameters are (units omitted): $A = 3687$, $\alpha = -0.0385$, $a = 0.511$, $\check{c}_1 = 2311, 2350, 2703$ (for constant, k^2-linear, inverse-square sound speed profile, respectively), $\delta = -0.0371$, $b = 1.405$, $\check{c}_0 = 4550$, and $\kappa = -0.04166$. For comparison purpose, the constant sound $\check{c}_1$ is taken to be the geometric mean of the inverse-square profile.

The solutions for $\tilde{p}_1(z)$ corresponding to various profiles shown above have been derived in literature, and may be summarized as follows [3]:

$$\tilde{p}_1(z) = \sqrt{\rho(z)} \begin{cases} e^{i\sigma z}, e^{-i\sigma z} & \text{constant}, \\ Ai(\eta(z)), Bi(\eta(z)), & k^2\text{-linear}, \\ \sqrt{\zeta(z)} H_\nu^{(1)}(\beta\zeta(z)), \sqrt{\zeta(z)} H_\nu^{(2)}(\beta\zeta(z)), & \text{inverse-square}, \end{cases} \tag{13}$$

where Ai, Bi are the Airy functions, and $H_\nu^{(1)}$, $H_\nu^{(2)}$ are the νth-order Hankel functions; relevant parameters/variables are defined below:

$$\eta(z) = -\frac{1}{\sqrt[3]{(\check{k}_1^2\delta)^2}} \left(\check{k}_1^2 \delta z + \check{k}_1^2 - \check{k}_0^2 \cos^2\theta_0 - \frac{\alpha^2}{4} \right), \tag{14}$$

$$\zeta(z) = 1 - \kappa z, \tag{15}$$

$$\sigma^2 = \frac{\alpha^2}{4} - \check{k}_1^2 \sin^2\theta_1, \tag{16}$$

$$\beta^2 = \frac{1}{\kappa^2}\left(\check{k}_0^2 b^2 - \check{k}_0^2 \cos^2\theta_0 - \frac{\alpha^2}{4}\right), \tag{17}$$

$$v^2 = \frac{1}{4} - \frac{\omega^2}{\kappa^2}\left(\frac{1}{\check{c}_1^2} - \frac{b^2}{\check{c}_0^2}\right) \tag{18}$$

with $\check{k}_1 = \omega/\check{c}_1$ and θ_1 defined as $\check{k}_1 \cos\theta_1 = \check{k}_0 \cos\theta_0$. It is to be noticed from Eq. (18) that for high frequency, or any other factor rendering v^2 negative, the Hankel function becomes imaginary orders. While both the Airy functions and the Hankel functions are generally built-in in most computational softwares, the imaginary order of Hankel functions may not be readily available, so that a special treatment may be needed [3]. For this instance, the authors have found that MATHEMATICA [25] is particularly useful in this analysis.

2.3. Reflection coefficient for an unperturbed seabed

According to the boundary perturbation theory [1], the same problem without seabed roughness constitutes the fundamental formulation for the study of the coherent field for the perturbed problem. Here, we establish the boundary operators based upon the solutions of the Helmholtz equations and boundary constraints discussed in the previous two sections.

For an incoming plane wave propagating in k_x direction, the solutions corresponding to Eqs. (1)–(4) may be expressed as

$$p_0(x,z) = A_0^-(k_x)\mathrm{e}^{-\mathrm{i}k_{0,z}z}\mathrm{e}^{\mathrm{i}k_x x}, \tag{19}$$

$$p_1(x,z) = [A_1^+(k_x)\mathscr{G}(k_x,z) + A_1^-(k_x)\mathscr{H}(k_x,z)]\mathrm{e}^{\mathrm{i}k_x x}, \tag{20}$$

$$\phi_2(x,z) = A_2^+(k_x)\mathrm{e}^{\mathrm{i}k_{2p,z}z}\mathrm{e}^{\mathrm{i}k_x x}, \tag{21}$$

$$\psi_2(x,z) = B_2^+(k_x)\mathrm{e}^{\mathrm{i}k_{2s,z}z}\mathrm{e}^{\mathrm{i}k_x x}, \tag{22}$$

where the vertical wavenumber $k_{i,z}$ in various layers are

$$k_{0,z}^2 = k_0^2 - k_x^2, \tag{23}$$

$$k_{2p,z}^2 = k_{2p}^2 - k_x^2, \tag{24}$$

$$k_{2s,z}^2 = k_{2s}^2 - k_x^2 \tag{25}$$

and $\mathscr{G}(k_x,z)$ and $\mathscr{H}(k_x,z)$ are one of the solution sets in Eq. (13), depending upon the sediment profile. The unknown amplitudes $A_i^{\pm}(k_x)$'s and $B_2^+(k_x)$ may be determined by the boundary conditions.

For convenience to adapt the variation of density and sound speed profiles in the sediment layer, the depth origin is taken to be in the center of the sediment layer. Applying the boundary conditions corresponding to Eqs. (5)–(9), with the seabed assumed to be flat interface, results in a linear system for the unknown amplitudes as

$$\tilde{\mathscr{B}}(k_x)\tilde{\chi}(k_x) = \tilde{\mathscr{C}}(k_x), \tag{26}$$

where $\tilde{\chi}(k_x)$ and $\tilde{\mathscr{C}}(k_x)$ are vectors defined as follows:

$$\tilde{\chi}(k_x) = [A_0^-(k_x)\ \ A_1^+(k_x)\ \ A_1^-(k_x)\ \ A_2^+(k_x)\ \ B_2^+(k_x)]^{\mathrm{T}}, \tag{27}$$

$$\tilde{\mathscr{C}}(k_x) = S_\omega \left[-\tfrac{1}{\mathrm{i}4\pi k_{0,z}}\ \ \tfrac{1}{\rho_1 \omega^2 4\pi}\ \ 0\ \ 0\ \ 0 \right]^{\mathrm{T}} \tag{28}$$

and $\tilde{\mathscr{B}}(k_x)$ is a matrix, which is

$$\tilde{\mathscr{B}}(k_x) = \begin{bmatrix} 1 & -\mathscr{G}(k_x,-h/2) & -\mathscr{H}(k_x,-h/2) & 0 & 0 \\ \frac{\mathrm{i}k_{0,z}}{\rho_1\omega^2} & \frac{1}{\rho_{1U}\omega^2}\mathscr{H}'(k_x,-h/2) & \frac{1}{\rho_{1U}\omega^2}\mathscr{G}'(k_x,-h/2) & 0 & 0 \\ 0 & \mathscr{G}(k_x,h/2) & \mathscr{H}(k_x,h/2) & \mu(2k_x^2-k_{2s,z}^2) & \mu 2k_x k_{2s,z}^2 \\ 0 & \frac{1}{\rho_{1L}\omega^2}\mathscr{G}'(k_x,h/2) & \frac{1}{\rho_{1L}\omega^2}\mathscr{H}'(k_x,h/2) & -\mathrm{i}k_{2p,z} & \mathrm{i}k_x \\ 0 & 0 & 0 & -2k_x k_{2p,z} & k_x^2-k_{2s,z}^2 \end{bmatrix}, \tag{29}$$

where ρ_{1U} (c_{1U}) and ρ_{1L} (c_{1U}) are, respectively, the density (sound speed) at the upper and the lower boundary of the sediment layer. Solutions of Eq. (26) yield the acoustic fields in various layers, including the reflection coefficient in the upper medium.

2.4. Coherent reflection from rough seabed

With the solutions for the unperturbed problem obtained in the previous section, the formulation for the coherent reflection from the rough surface may be derived through boundary perturbation method. Following the theory developed by Kuperman and Schmidt [1], the effects of roughness on the coherent field may be represented by several operators accounting for surface elevation and orientation. Since the theory and formulation are well documented in the literature, there is no need to repeat here. In this section, we merely present the particular formalisms and operators relevant to present analysis.

The derivation using boundary perturbation method leads to the following modified linear system for the coherent field, as opposed to Eq. (26) for the unperturbed seabed:

$$\left[\tilde{\mathscr{B}}(k_x) + \frac{\langle \gamma^2 \rangle}{2} \frac{\partial^2}{\partial z^2} \tilde{\mathscr{B}}(k_x) + \tilde{I}(k_x) \right] \langle \tilde{\chi}(k_x) \rangle = \tilde{\mathscr{C}}(k_x), \tag{30}$$

where $\langle \gamma^2 \rangle$ is the mean-squared roughness, and $\tilde{I}$ is a scattering operator given by

$$\begin{aligned} \tilde{I}(k_x) = & -\frac{\langle \gamma^2 \rangle}{\sqrt{2\pi}} \int \mathrm{d}q\, P_b(q-k_x) \left[\frac{\partial}{\partial z} \tilde{\mathscr{B}}(q) - \mathrm{i}(k_x - q) \circ \tilde{b}(q) \right] \\ & \times \tilde{\mathscr{B}}^{-1}(q) \left[\frac{\partial}{\partial z} \tilde{\mathscr{B}}(k_x) - \mathrm{i}(q-k_x) \circ \tilde{b}(k_x) \right], \end{aligned} \tag{31}$$

where P_b is the power spectrum of the rough surface, and the operation $\circ$ is either inner or outer product, depending upon the types of boundary condition; the details of the formulation should be referred to the original paper [1].

Relevant operators appearing in Eqs. (30) and (31) are

$$\frac{\partial}{\partial z}\tilde{\mathscr{B}}(k_x) = \begin{bmatrix} -\mathrm{i}k_{0,z} & -\mathscr{G}'(k_x,-h/2) & -\mathscr{H}'(k_x,-h/2) & 0 & 0 \\ \frac{k_{0,z}^2}{\rho_1\omega^2} & \frac{1}{\rho_{2U}\omega^2}\mathscr{G}''(k_x,-h/2) & \frac{1}{\rho_{2U}\omega^2}\mathscr{H}''(k_x,-h/2) & 0 & 0 \\ 0 & \mathscr{G}'(k_x,h/2) & \mathscr{H}'(k_x,h/2) & \mathrm{i}k_{2p,z}\mu(2k_x^2-k_{2s}^2) & 2\mathrm{i}\mu k_x k_{2s,z}^2 \\ 0 & \frac{1}{\rho_{2L}\omega^2}\mathscr{G}''(k_x,h/2) & \frac{1}{\rho_{2L}\omega^2}\mathscr{H}''(k_x,h/2) & k_{2p,z}^2 & -k_x k_{2s,z} \\ 0 & 0 & 0 & 2k_x k_{2p,z}^2 & -(k_x^2 k_{2s,z}-k_{2s,z}^3) \end{bmatrix}, \tag{32}$$

$$\frac{\partial^2}{\partial z^2}\tilde{\mathscr{B}}(k_x) = \begin{bmatrix} -k_{0,z}^2 & -\mathscr{G}''(k_x,-h/2) & -\mathscr{H}''(k_x,-h/2) & 0 & 0 \\ \frac{\mathrm{i}k_{0,z}^3}{\rho_1\omega^2} & \frac{-1}{\rho_{2U}\omega^2}\mathscr{G}'''(k_x,-h/2) & \frac{-1}{\rho_{2U}\omega^2}\mathscr{H}'''(k_x,-h/2) & 0 & 0 \\ 0 & \mathscr{G}''(k_x,h/2) & \mathscr{H}''(k_x,h/2) & -\mu(2k_x k_{2p,z}^2-k_{2s}^2 k_{2p,z}^2) & -2\mu k_x k_{2s,z}^3 \\ 0 & \frac{1}{\rho_{2L}\omega^2}\mathscr{G}'''(k_x,h/2) & \frac{1}{\rho_{2L}\omega^2}\mathscr{H}'''(k_x,h/2) & \mathrm{i}k_{2p,z}^3 & -\mathrm{i}k_x k_{2s,z}^2 \\ 0 & 0 & 0 & -2k_x k_{2p,z}^3 & k_x^2 k_{2s,z}^2 - k_{2s,z}^4 \end{bmatrix}, \tag{33}$$

$$\tilde{b}(k_x) = \begin{bmatrix} \frac{-\mathrm{i}k_x}{\rho_1\omega^2} & \frac{\mathrm{i}k_x}{\rho_2 U\omega^2}\mathscr{G}(k_x,-h/2) & \frac{-\mathrm{i}k_x}{\rho_{2U}\omega^2}\mathscr{H}(k_x,-h/2) & 0 & 0 \\ 0 & 0 & 0 & 0 & 0 \\ 0 & 0 & 0 & 0 & 0 \\ 0 & 0 & 0 & 0 & 0 \\ 0 & 0 & 0 & 0 & 0 \end{bmatrix}, \tag{34}$$

where the superscript $'$ is the derivative with respect to z. The linear system, Eq. (30), may now be solved for $\langle\tilde{\chi}\rangle$ to obtain the coherent fields.

3. Results and discussion

The above formulations may be numerically implemented to show the effects of various parameters on the coherent reflection field. Since there are numerous variables and parameters in the problem, some of them are taken to be constant values, e.g., $c_0 = 1500$ m/s,

$\rho_0 = 1000\ \mathrm{kg/m^3}$. For the seabed roughness, the Goff–Jordan power-law spectrum [26] is employed:

$$P_b(k) = \frac{4k_*^3}{(k^2 + k_*^2)^2}, \tag{35}$$

where k_* represents a characteristic wavenumber of the rough surface.

To ensure the correctness of the numerical algorithms, the following results, when possible, have been asymptotically compared with those generated by current existing software OASES [27], and were found a good agreement. A more detailed discussion regarding the benchmarking procedure of the numerical results may be found in Ref. [2].

Fig. 3 shows the coherent reflection coefficients at frequency $f = 100$ Hz for the seabed environment shown in Fig. 2; the numerical values for various parameters are shown in the legend, and the solid, dashed, dotted curves correspond to inverse-square, k^2-linear, and constant sound speed profile, respectively. It is noted that the sediment thickness $h = 30$ m is twice of the acoustic wavelength, and the acoustic properties (e.g., compressional sound speed) vary substantiously throughout the sediment layer. Under this situation, the coherent reflection coefficients corresponding to the different profiles demonstrate a quite different results. In general, the inverse-square sound speed profile yields smaller coherent reflection coefficients. Since these are the results corresponding to three different environmental models, their comparisons may not be justified without a common ground. However, the distinctive results for various sediment profiles clearly indicated that the modelling of sediment layer is an important process in the study of seabed acoustics.

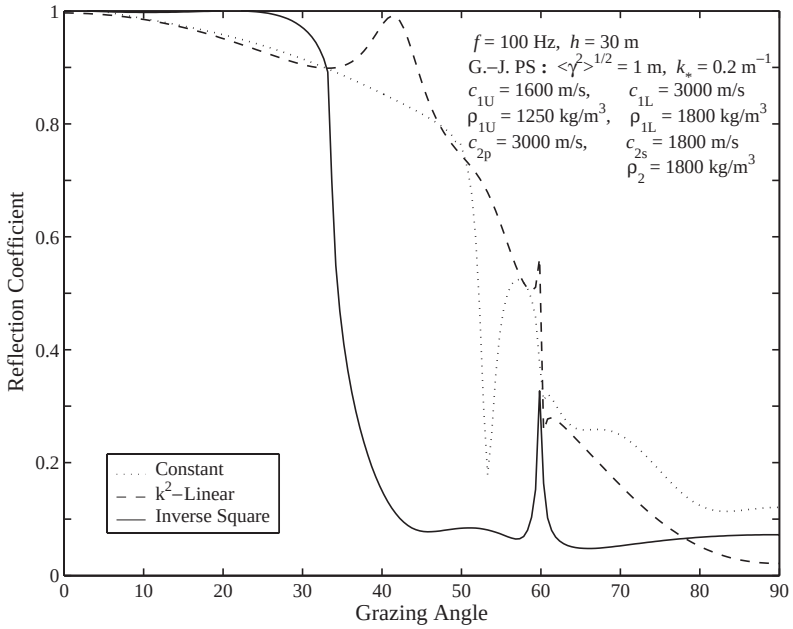

Fig. 3. Coherent reflection coefficient for frequency 100 Hz.

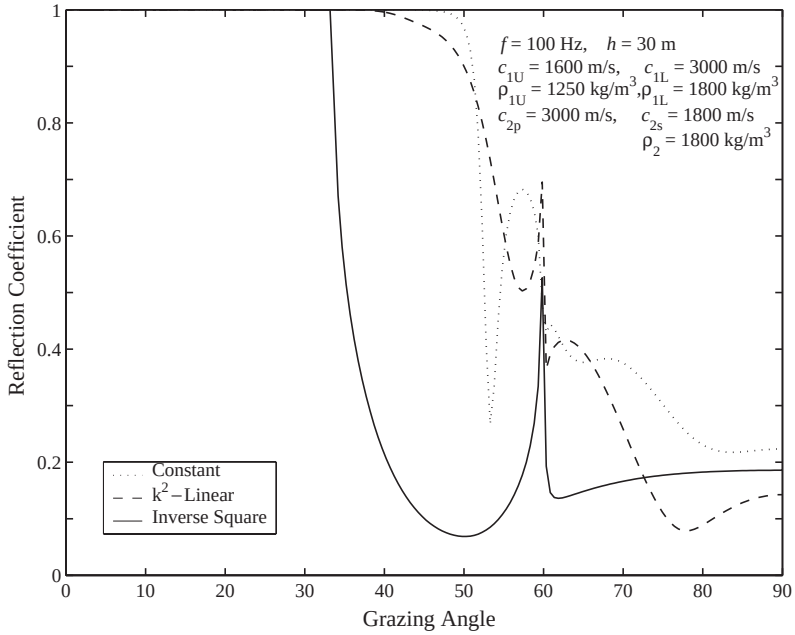

Fig. 4. Coherent reflection coefficient for frequency 100 Hz for smooth seabed.

A few special features in Fig. 3 should also be noted. The spike appearing at 60° is obviously due to compressional sound speed, at which the compressional wave reaches total reflection. Below this angle, energy continues to penetrate into the basement through shear waves and rough surface scattering, so that the total reflection does not occur. The oscillatory behavior reflects the degree of contrast in acoustic properties between various layers, and the constant sound speed seems to have a highest contrast in this case. Furthermore, the present analysis concerns the reflection under the effects of seabed roughness. In this regard, Fig. 3 is to compare with Fig. 4, where the seabed roughness is suppressed. A comparison between Figs. 3 and 4 reveals that the coherent reflection coefficient for the smooth seabed is generally higher than that for rough seabed; moreover, the coefficient reaches unity value at the angle corresponding to shear wave in the sea basement, which is about $\cos^{-1}(1500/1800) \simeq 34^\circ$ in the present case. These results clearly show that the seabed roughness diverts energy away from the specular direction, therefore, reducing coherent energy as expected.

Figs. 5 and 6 are the results for the same environmental parameters as Fig. 3, except now the frequency is 30 and 120 Hz, respectively. At low frequency, e.g., 30 Hz (wavelength 50 m), the coherent reflection coefficient is generally higher than that for high frequency, e.g., 120 Hz. Moreover, for low frequency, the total reflection nearly occurs when the shear critical angle arrives. These are all due to the fact that the seabed roughness becomes less importance when the frequency is lowered. At high frequency, the coherent reflection coefficient is greatly reduced, and the behavior of the curves shows the details of the structure of the layering media.

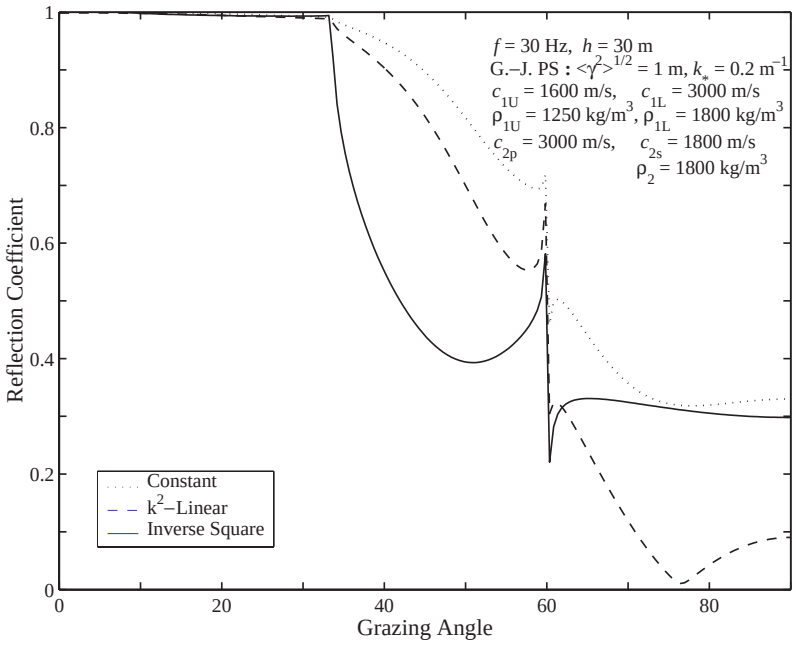

Fig. 5. Coherent reflection coefficient for frequency 30 Hz.

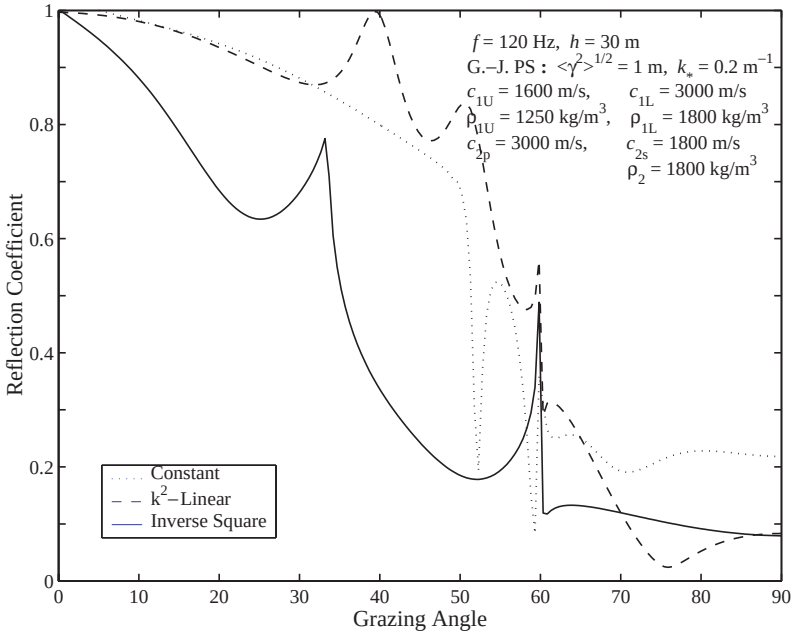

Fig. 6. Coherent reflection coefficient for frequency 120 Hz.

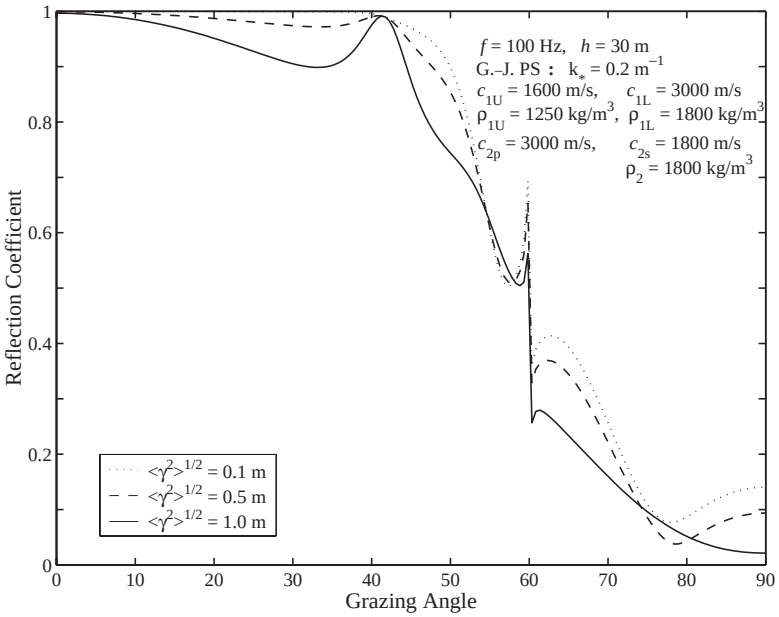

Fig. 7. Coherent reflection coefficient for k^2-linear sound speed profile in the sediment layer, and three values of r.m.s. seabed roughness.

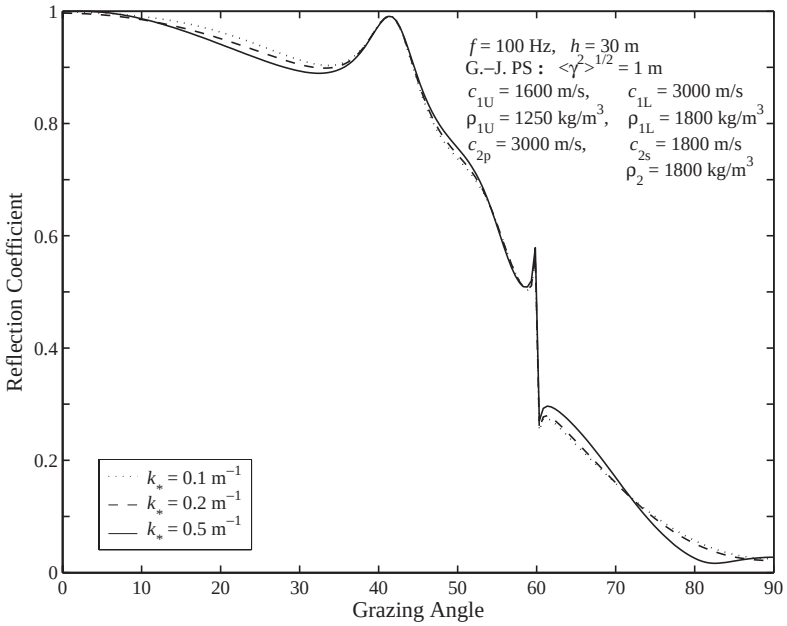

Fig. 8. Coherent reflection coefficient for k^2-linear sound speed profile in the sediment layer, and three values of characteristic wavenumber of the seabed roughness.

The magnitude of r.m.s. seabed roughness is expected to directly affect the coherent reflection coefficient: the larger the magnitude (i.e., larger Rayleigh parameter, which is defined as $\mathscr{P} = 2k_0\sqrt{\langle\gamma^2\rangle}\cos\theta$), the stronger the scattered field, and thus the smaller the reflection coefficient,

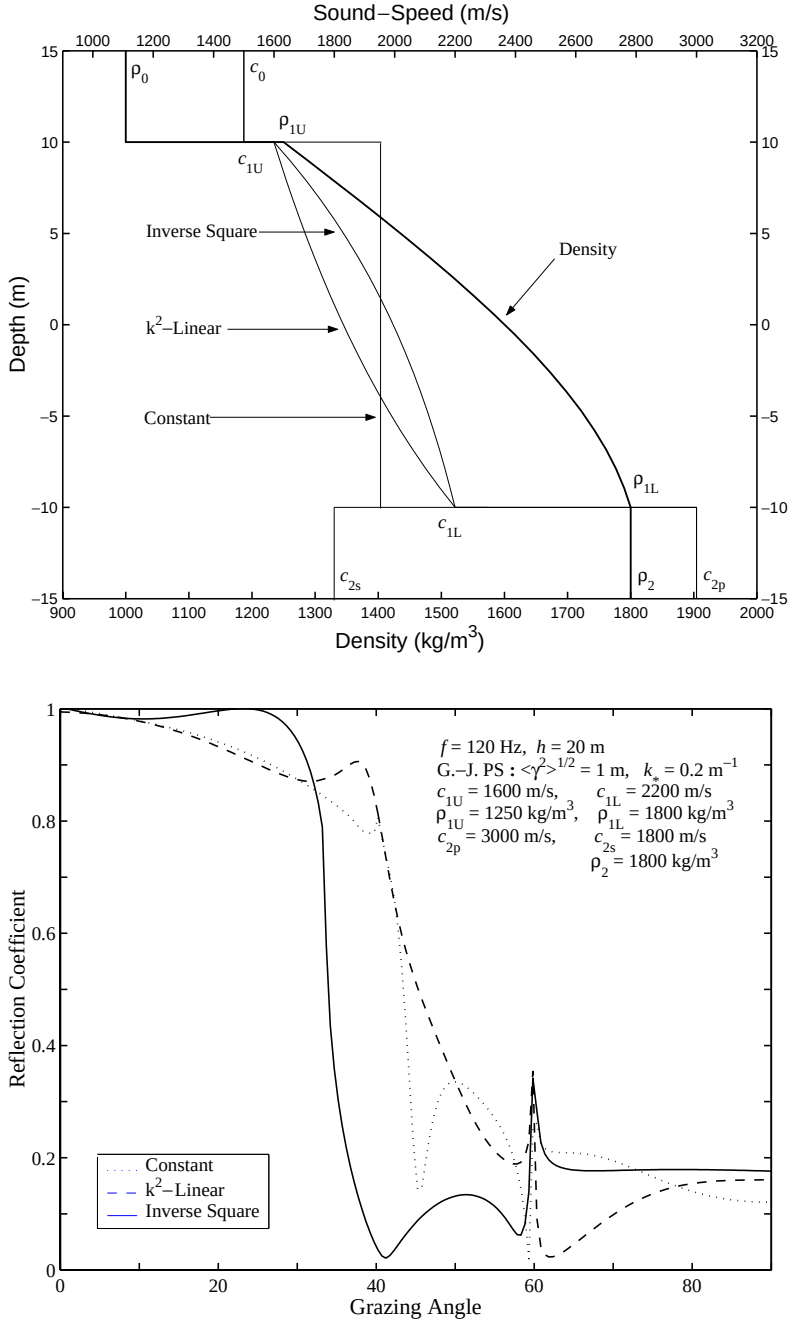

Fig. 9. Coherent reflection coefficient for the environment shown in the upper figure.

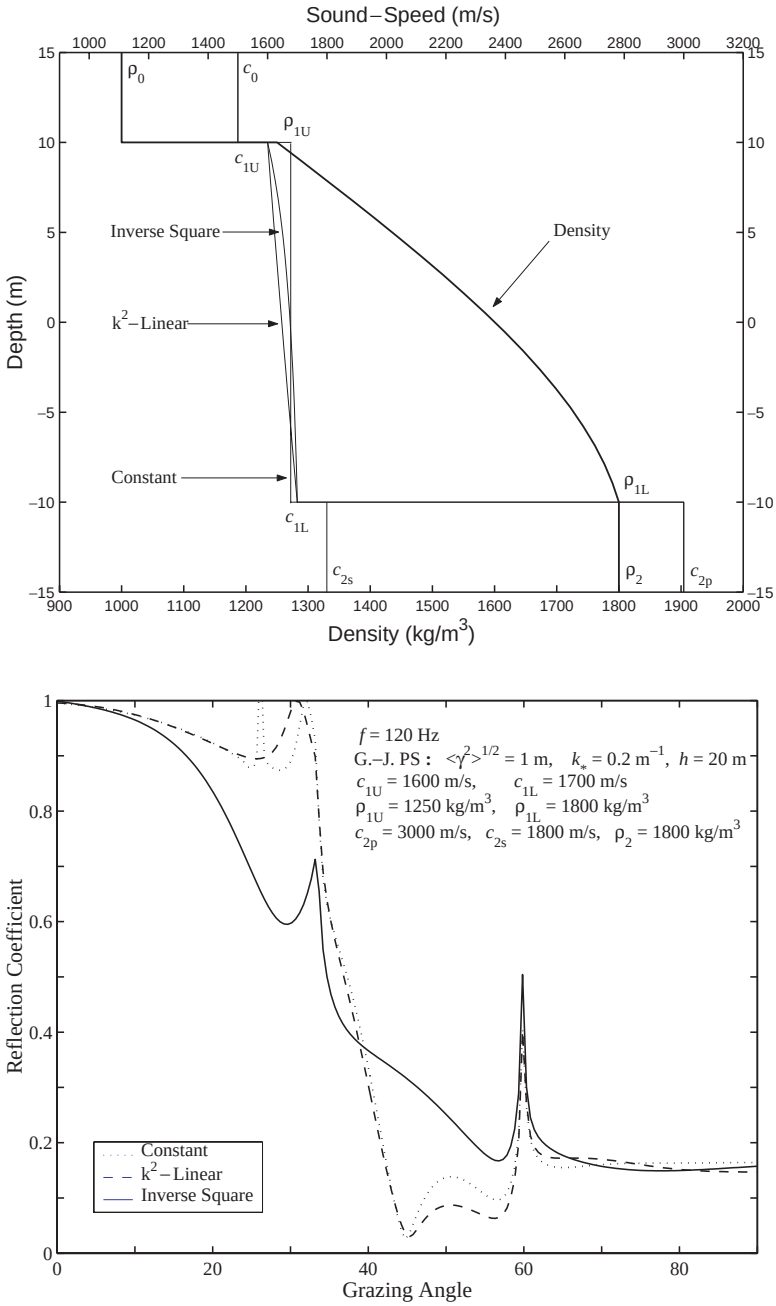

Fig. 10. Coherent reflection coefficient for the environment shown in the upper figure.

Fig. 7 shows the coherent reflection coefficient for k^2-linear sound speed profile in the sediment layer, and three values of r.m.s. roughness on seabed. The results indicate that the coherent reflection coefficient decreases as r.m.s. roughness increases as expected; others profiles should also yield similar results.

On the other hand, the characteristic wavenumber (or equivalently the correlation length) of the seabed roughness may have only a minor effect on the coherent field. Fig. 8 shows the results for three values of the characteristic wavenumber. It is seen that the three curves are close to each other, with only a slight difference at the higher and lower incident angles. These results are reminiscent of the fundamental principles that the coherent field, being an ensemble average of the total random field, mainly depends upon the gross structure of the rough surface, which is represented by the r.m.s. roughness. The details of the roughness distribution represented by the characteristic wavenumber, though important with respect to the scattered field as might be expected, plays little role for the coherent field.

Finally, the coherent reflection coefficients corresponding to two other representative sound speed distributions and sediment thicknesses are shown in Figs. 9 and 10 for frequency 120 Hz; here, the sediment thickness is 20 m, and the sound speed at the lower boundary of the sediment layer has a step jump with respect to the basement. These two figures show that, as the sound speed profiles get closer to each others, the coherent reflection coefficients also get closer, particularly in the range of high grazing angles; however, there still shows substantial difference between the results for the inverse-square profile with those corresponding to the other two, indicating that it is important to employ the appropriate model for the sediment layer in the study of seabed acoustics. It is also noted that, in Fig. 10, there exists a spike near $\cos^{-1}(1600/1800) \simeq 27^{\circ}$ in the dotted curve, reflecting the strong sound speed contrast between the isovelocity sediment layer and the basement.

4. Conclusions

In this paper, we have studied the coherent reflection of an acoustic plane wave from a rough seabed with a continuously varying density and sound speed in the sediment layer overlying a semi-infinite uniform elastic basement. The analysis combines the analytical solutions of the Helmholtz equation in the sediment layer with a formalism based upon boundary perturbation method to treat rough surface scattering. Numerical algorithms assisted by the current software such as MATHEMATICA to deal with the special functions are developed to generate the coherent reflection coefficients. The study offers a realistic model for the seabed environment, and is useful in the simulation of seabed acoustics.

A generalized exponential density profile joined with one of the three classes of sound speed profiles, including constant, k^2-linear, and inverse-square, are employed and analyzed. The results for the coherent reflection coefficients have shown that the variation of sound speed inside the sediment layer may have a great influence on the coherent reflection field. Even only with a few percent discrepancies, the k^2-linear and inverse-square profiles still produce a discernible difference in the coherent reflection coefficients. This indicates that the correct use of the sediment profile is important in the modelling of seabed acoustics.

This study, although develops no new theory, provides a succinct formulation for the study of the coherent reflection from a rough seabed, and yields many useful results. Extension of the present analysis may consider to include shear property in the sediment layer, for which the analytical solutions for the Helmholtz equation still await for further investigation.

Acknowledgements

This work has been supported in part by the National Science Council of Taiwan, R.O.C. through contract NSC90-2611-E-110-009 and in part by the Ministry of Education through the joint program between National Cheng-keng University and National Sun Yat-sen University. The authors would like to express our profound thanks for their financial supports.

References

[1] W.A. Kuperman, H. Schmidt, Self-consistent perturbation approach to rough surface scattering in stratified elastic media, *Journal of the Acoustical Society of America* 86 (1989) 1511–1522.
[2] J.-Y. Liu, C.-C. Wang, C.-F. Huang, Coherent reflection from a rough interface over an inhomogeneous transition fluid layer, *Journal of Computational Acoustics* 8 (3) (2000) 401–414.
[3] A.J. Robins, Reflection of plane acoustic wave from a layer of varying density, *Journal of the Acoustical Society of America* 87 (4) (1990) 1546–1552.
[4] A.J. Robins, Reflection of a plane wave from a fluid layer with continuously varying density and sound speed, *Journal of the Acoustical Society of America* 89 (4) (1991) 1686–1696.
[5] A.J. Robins, Exact solutions of the Helmholtz equation for plane wave propagation in a medium with variable density and sound speed, *Journal of the Acoustical Society of America* 93 (3) (1993) 1347–1352.
[6] H. Schmidt, SAFARI: Seismic-acoustic fast field algorithm for range independent environment. User's Guide, Report SR-113, SACLANT Undersea Research Centre, La Spezia, Italy, 1988.
[7] H. Schmidt, F.B. Jensen, A full wave solution for propagation in multilayered viscoelastic media with application to Gaussian beam reflection at fluid–solid interfaces, *Journal of the Acoustical Society of America* 77 (1985) 813–825.
[8] L.B. Dozier, F.D. Tappert, Statistics of normal mode amplitudes in a random ocean, *Journal of the Acoustical Society of America* 64 (1978) 533–547.
[9] M.B. Porter, E.L. Reiss, A numerical method for ocean acoustic normal modes, *Journal of the Acoustical Society of America* 76 (1984) 244–252.
[10] M.B. Porter, The KRAKEN normal mode program, Report SM-245, SACLANT Undersea Research Centre, La Spezia, Italy, 1991.
[11] M.D. Collins, A split-step Padé solution for the parabolic equation method, *Journal of the Acoustical Society of America* 93 (1993) 1736–1742.
[12] F.D. Tappert, The parabolic approximation method, in: J.B. Keller, J.S. Papadakis (Eds.), *Wave Propagation in Underwater Acoustics*, Springer, Berlin, 1977, pp. 224–287.
[13] F.B. Jensen, W.A. Kuperman, M.B. Porter, H. Schmidt, *Computational Ocean Acoustics*, AIP Press, College Park, MD, 2000.
[14] P. Epstein, Reflections of waves in an inhomogeneous absorbing medium, *Proceedings of the National Academy of Sciences USA* 16 (1930) 627.
[15] A.O. Williams, D.R. MacAyeal, Acoustic reflection from a sea bottom with linearly increasing sound speed, *Journal of the Acoustical Society of America* 66 (1979) 1836–1841.
[16] L.M. Brekhovskikh, *Waves in Layered Media*, Academic Press, New York, 1980.
[17] J. Lekner, Reflection and transmission of compressible waves: some exact results, *Journal of the Acoustical Society of America* 87 (6) (1990) 2325–2331.
[18] C. Ranz-Guerra, R. Carbo-Fite, Impulse response of sediment layers with variable density gradients, in: *Acoustics and the Sea Bed*, Bath U.P., Bath, England, 1983.
[19] S.R. Rutherford, K.E. Hawker, Effect of density gradients on bottom reflection loss for a class of marine sediments, *Journal of the Acoustical Society of America* 63 (1978) 750–757.
[20] I. Tolstoy, The theory of waves in stratified fluids including the effects of gravity and rotation, *Reviews in Modern Physics* 35 (1963) 207–230.

[21] I. Tolstoy, Effects of density stratification on sound waves, *Journal of Geophysical Research* 70 (24) (1965) 6009–6015.
[22] A.J. Robins, Generation of shear and compression waves in an inhomogeneous elastic medium, *Journal of the Acoustical Society of America* 96 (3) (1994) 1669–1676.
[23] E.L. Hamilton, Geoacoustic modeling of the sea floor, *Journal of the Acoustical Society of America* 68 (1980) 1313–1340.
[24] J. Miklowitz, *The Theory of Elastic Waves and Waveguides*, North-Holland, Amsterdam, 1978.
[25] S. Wolfram, *The Mathematica Book*, 3rd Edition, Cambridge University Press, Cambridge, 1996.
[26] J.A. Goff, T. Jordan, Stochastic modeling of seafloor morphology: inversion of Sea Beam data for second-order statistics, *Journal of Geophysical Research* 93 (13) (1988) 589–513, 608.
[27] H. Schmidt, *OASES: Ocean Acoustics Seismic Exploration Synthesis, User's Guide and Reference Manual, Version* 3.1, 2002.